frontiers in Materials

ORIGINAL RESEARCH
published: 21 February 2022
doi: 10.3389/fmats.2022.844608

Strength Analysis and Optimization of Alkali Activated Slag Backfills Through Response Surface Methodology

Xinghang Dai[1], *Lei Ren*[2], *Xiaozhong Gu*[2], *Erol Yilmaz*[3], *Kun Fang*[2,3]* *and Haiqiang Jiang*[2]*

[1]School of Civil Engineering, Liaoning Petrochemical University, Fushun, China, [2]Key Laboratory of Ministry of Education on Safe Mining of Deep Metal Mines, Northeastern University, Shenyang, China, [3]Department of Civil Engineering, Geotechnical Division, Recep Tayyip Erdogan University, Fener, Turkey, [4]Department of Civil Engineering, Lakehead University, Thunder Bay, ON, Canada

The significant difference in water-to-binder ratio, activator type and concentration between alkali-activated slag (AAS) paste/mortar/concrete and AAS-based cemented paste backfill (AAS-CPB) means that previous results related to the properties and mix optimization of AAS materials cannot be directly translated to AAS-CPB. This study statistically identifies the effect of key influential variables such as silicate modulus, slag fineness and activator concentration on 3- and 28 day unconfined compressive strength (UCS) of AAS-CPB by central composite design (CCD) established in response surface methodology (RSM). In this study, the prominence of independent variables and their relations are investigated by using ANOVA (analysis of variance) having a significant level of 0.05. ANOVA results certify that there is a strong link between the level of variable contribution on UCS performance of AAS-CPB and curing age. Obviously, silicate modulus and activator concentration are the most major variables influencing UCS at 3 and 28 days, respectively. Increased fineness of slag and higher pH of pore solution enhance 3 day UCS, but restrain the further hydration of unreacted slag and subsequent the gain in strength at advanced curing ages. The combination of independent variables of silicate modulus (0.295), slag fineness (12630.2), activator concentration (0.45) gives the optimum responses.

Keywords: tailings, alkali activated slag backfill, strength development, response surface methodology, activator type, slag fineness

OPEN ACCESS

Edited by:
Huisu Chen,
Southeast University, China

Reviewed by:
Lijie Guo,
Beijing General Research Institute of Mining and Metallurgy, China
Xiaojun Zhu,
Anhui University, China

***Correspondence:**
Kun Fang
kfang078@uottawa.ca
Haiqiang Jiang
jianghaiqiang@mail.neu.edu.cn

Specialty section:
This article was submitted to Structural Materials, a section of the journal Frontiers in Materials

Received: *28 December 2021*
Accepted: *04 February 2022*
Published: *21 February 2022*

Citation:
Dai X, Ren L, Gu X, Yilmaz E, Fang K and Jiang H (2022) Strength Analysis and Optimization of Alkali Activated Slag Backfills Through Response Surface Methodology. Front. Mater. 9:844608. doi: 10.3389/fmats.2022.844608

1 INTRODUCTION

Mining activities and ore processing are closely linked by the generation of considerable volumes of underground voids and mine tailings, respectively (Benzaazoua et al., 2004; Hajkowicz et al., 2011). If not managed properly, these voids and tailings can bring about severe and long-term operational (e.g., ground or strata instability) (Jafari et al., 2021), environmental (e.g., heavy metal pollution) (Koohestani et al., 2018) and geotechnical risks (e.g., tailings dam failure and subsidence) (Rana et al., 2021). In recent years, technological progresses coupled with environmental regulation changes, including cemented paste backfill (CPB) system, have also triggered the development in tailings and voids management (Benzaazoua et al., 1999; Fall et al., 2010). Recycling mine tailings into underground mined-out voids, CPB has been well accepted by the mining industry as one of the most effective systems for handling tailings and underground voids (Fall et al., 2008; Ercikdi et al., 2009b; Yilmaz et al., 2011). CPB is mainly a homogeneous material formed by uniformly blending

mine tailings, hydraulic binders and mixing water in a certain mass ratio (Helinski et al., 2007; Simms and Grabinsky, 2009). Mine tailings, the fine-grained and uneconomic residue of ore processing plant, is used at a typical solid concentration of 75-85wt.% for making CPB (Ercikdi et al., 2013; Ouattara et al., 2018) while mixing water, the water recycled from the plant or municipal water, is used at a typical content of 15-25wt.% to reach a desirable CPB slump required for its delivery to underground mined-out stopes (Zhao et al., 2020). The yield stress and mechanical strength of CPB are intensely affected by the type and quality of mine tailings and mixing water employed for preparing CPB materials (Kesimal et al., 2003; Simon and Grabinsky, 2013; Wu et al., 2015; Jiang and Fall 2017). Besides, the general use or ordinary Portland cement (also known as OPC) is most often used as a typical hydraulic binder within CPB's production for its versatility and availability (Ercikdi et al., 2009a; Tariq and Yanful, 2013).

While numerous works have been completed so far on mortar and concrete (Rakhimova and Rakhimov, 2015), relatively little work for the enhanced CPB performance has been done by the use of new lab tool and materials. There are some clear differences between CPB, mortar and concrete (Benzaazoua et al., 2004). Fresh and hardened characteristics of CPB is quite different from those of mortar and concrete (Li et al., 2021). This means that the amount of the water used within CPB is far more than the chemical binding capability of OPC within CPB, thereby leading to slow acquisition in the strength and low strength, especially for early ages. Moreover, mine fill cost as a percentage of the investment of the mining operation accounts for about 20%, and OPC takes up to 75% of the paste backfill costs (Belem and Benzaazoua, 2008). The usage and manufacture of OPC ingests quantities of natural resources while discharging a large amount of carbon dioxide (CD) to air (Turner and Collins, 2013). As stated by statistics, making 1-ton cement consumes 1.5-ton raw resources and produces 0.8-ton CD simultaneously (Ahmari et al., 2012; Jiang et al., 2019). All of these disadvantages have prompted the mining industry to seek for less expensive and environmental-friendly alternative binders (Behera et al., 2021).

In recent years, alkali-activated slag (AAS) materials, a new low-carbon cementitious material, have attracted increasing attention in the concrete industry (Aydin and Baradan, 2012; Bilim et al., 2013; Yuan et al., 2015; Gebregziabiher et al., 2016; Abdollahnejad et al., 2019). AAS is produced by activating slag additive with different types of activator (El-Wafa and Fukuzawa, 2018; Yang J. et al., 2019). Typical activators used for AAS are alkali hydroxide, silicate, carbonate or sulfate (Cihangir et al., 2015; Luukkonen et al., 2018; Korde et al., 2019). Recent research results show that compared with OPC-based CPB (OPC-CPB), AAS-based CPB (AAS-CPB) have excellent properties such as better-quality fluidity (Koohestani et al., 2021; Zaibo et al., 2021; Zhang et al., 2021), higher mechanical strength (Cihangir et al., 2018; Jiang et al., 2020; Cavusoglu et al., 2021), and better sulfate corrosion resistance (Cao et al., 2019b; Zhu et al., 2021b; Zheng et al., 2021). In addition, a recent study showed that usage of AAS in mine backfill fabrication can reduce the cementing cost up to 35% (Saedi et al., 2019). To sum up, AAS materials have great potential to serve as promising alternative to OPC within CPB production (Guo et al., 2021). Formulation and optimization of AAS binder is an important subject in the design of CPB (Sun et al., 2019). Several works suggest that the characteristics of AAS-CPB are significantly influenced by the sort and dosage of activator (Cihangir et al., 2015; Cihangir et al., 2018; Jiang et al., 2019; Rena et al., 2022) as well as slag characteristics (Xue et al., 2020). This means that the mixture proportion design of AAS-CPB is a complex multi-variable optimization system (Fall et al., 2008). Nevertheless, AAS-CPB materials have been classically expressed by trial and error method to obtain the anticipated properties for a given curing time and CPB mix recipe (Zhang and Yue, 2018; Yang et al., 2020). Such methods often require massive workloads, which are often unsatisfactory due to the neglect of interactions between components (Zhou et al., 2020).

There are some methods dealing the effect of several features on laboratory-based target variable (Köken and Lawal, 2021). One of them is to use response surface methodology (RSM) which uses the multivariate nonlinear regression method and strive for the optimal experimental conditions (Oraon et al., 2006; Palanikumar, 2007; Soto-Pérez et al., 2015). Being one of the most entirely used experimental design ways, RSM uses central composite design (CCD) for appraising the link between autonomous factors and responses (Zhu et al., 2021a). Recent work has indicated that the amount of OPC and silica fume to have concrete's desired unconfined compressive strength (UCS) is optimized by using the CCDs with RSM (Anurag et al., 2021). Time-dependent effect on the design of cementitious materials incorporating fly ash and iron oxide as mineral additives has been also optimized by using the RSM analysis (Gao et al., 2016).

Several works (e.g. Dai et al., 2019; Sun et al., 2020; Hefni and Hassani, 2021) have been done on CPB materials through the RSM technique. Nevertheless, none of them mentions the effect of silicate modulus, slag fineness and activator concentration on 3- and 28 day UCS of AAS-CPB. To fill this information gap, an extensive work on AAS-CPB samples by taking into account the most inducing factors leading to high UCS values at 3 and 28 days was carried out using the RSM analysis. A combination of experimental design and analytical modeling was also utilized for offering the best mixture ratios for AAS-CPB samples.

2 MATERIALS AND METHODS

2.1 Materials

2.1.1 Tailings

Silica-based tailings (ST) having a silicon dioxide of 98.6wt.% was employed for making CPB samples. Due to the fact that mine tailings (MT) chemistry is relatively complex and have a profound effect on the testing results, it is critical to use ST as aggregate material within CPB. This will eventually eradicate hesitations in the outcomes of MT-based CPB materials (Cao et al., 2019a). Indeed, it is pertinent to note that the grain size distribution (GSD) of ST consisting mainly of quartz (most prevalent mineral on Earth) is fairly akin to the mean GSD of MT found in most modern hard rock mines worldwide (Jafari et al., 2020). **Figure 1** presents the cumulative GSD curves of ST material which is wet analyzed on Malvern Panalytical Mastersizer laser diffraction test device coupled with a Hydro

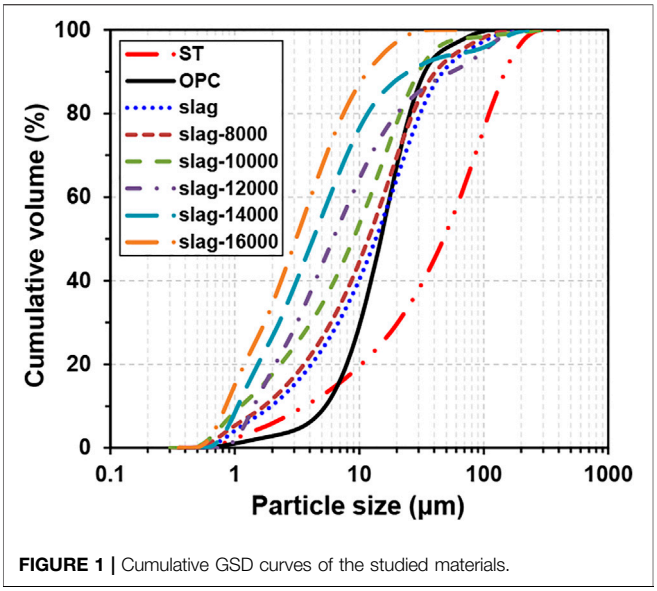

FIGURE 1 | Cumulative GSD curves of the studied materials.

S dispersion unit of a 150 ml capacity). The measurement of GSD points that the tailings sample has contained 28.41% particle size smaller than 20 μm. **Table 1** also lists the fundamental physical characteristics of ST considered as artificial tailings in this study.

2.1.2 Binder Materials

The binder used in this experiment includes an AAS binder and a typical commercial p O 42.5R OPC which is used as a reference. Slag was ensured by an iron-steel plant situated in Hubei province, China, in powder form. **Table 2** points out the main oxide and physical analyses of as-received slag and OPC. It is apparent that specific gravity (SG), specific surface area (SSA) and uniformity coefficient of OPC and as-received slag materials are respectively 3.3, 5,808 cm^2/g, and 3.29, and 2.87, 7,251 cm^2/g, and 9.11. GSD of as-received slag appears to be finer than that of OPC (**Figure 1**). X-ray diffraction (XRD) displays that slag exhibits a wide-peak package between (2θ) 25° and 35°, indicating that slag is almost completely vitreous with an amorphous structure (**Figure 2**). To appraise the influence of slag fineness on UCS performance of AAS-CPB, as-received slag was ground to BET-based SSA values of 8,073, 10,056, 11,934, 14,065 and 15,932 cm^2/g, respectively, using a ball mill. Note that Brunauer, Emmett and Teller (BET) theory is employed for assessing gas adsorption data and creating a SSA result stated in cm^2/g. The obtained slag materials are designated as slag-8,000, slag-10,000, slag-12,000, slag-14,000 and slag-16,000. The GSD curves of these grinded slags are shown in **Figure 1**.

2.1.3 Activators

Alkaline activator used was a mix of water glass (WG) solution (SiO_2 = 29.3%; Na_2O = 12.7%; H_2O = 58.0%) and sodium hydroxide (SH) with >99% purity. SH and WG were mixed in various proportions to obtain alkaline activators with silicate modulus (SiO_2 to Na_2O ratio by mass) in the range of 0.26–0.42. WG's density and pH values are respectively 1,490 kg/m^3 and 12.5. The mixing water considered in this study was de-ionized water. Details on activator's preparation can be found elsewhere 35.

2.2 Specimen Manufacturing and UCS Testing

Total 102 AAS-CPB specimens in triplicate were manufactured by mixing ST, slag, alkali activator and water for about 10 min in a double spiral blender. Prior to mixing, ST and slag were agitated by hand for 1 min. The solid concentration and slag dosage of all mixtures were set to 75% and 6%, respectively. Homogenized AAS-CPB samples were cast into plastic cylindrical molds having *D*×*H*: 50 × 100 mm. Note that there is no perforated hole at the bottom of molds for drainage purposes. The cylindrical molds were then capped with lids and maintained in a cure room holding 20 ± 1°C temperature and 95% moisture until 28 days. Following the desired cure period, the UCS tests of AAS-CPB samples were done by using a full automatic press (i.e., Humboldt HM-5030; 50 kN capacity). UCS test was done at a stress rate of 1 mm per minute until specimen fails under stress application. Before testing, CPB was taken out from the curing chamber and levelled with flat and parallel end surfaces for UCS testing. Note that the final result was calculated by averaging the results of three diverse UCS tests.

2.3 Experimental Design and Statistical Analysis

It has been reported that silicate modulus, slag fineness, activator concentration and curing temperature are the key influencing factors in the hydration of AAS binder. Since the slag nature and curing temperature are uncontrolled variables, silicate modulus, slag fineness and activator concentration (alkali activator/slag by mass) were selected as independent variables and are labeled x_1, x_2 and x_3. UCS at 3 and 28 days were taken as the response variables. Being the most frequently utilized RSM design, CCC was adopted to design the experiment. The effects of each independent variable were assessed at five levels, with the coded values of -alpha, −1, 0, +1, +alpha (**Table 3**), resulting in seventeen different experimental runs with three replicates at the center points. The spatial distribution of these experimental runs is illustrated in **Figure 3**. The levels of the variables were

TABLE 1 | A summary of physical characteristics of the studied ST material.

Type/ element	D_{10} (μm)	D_{30} (μm)	D_{50} (μm)	D_{60} (μm)	Fines (-20 μm, %)	Uniformity coefficient C_u	Curvature coefficient C_c	Specific gravity (–)	Specific surface (cm^2/g)
ST	3.66	20.4	38.8	63.7	29.6	17.4	1.79	2.65	4,238

$C_u = D_{60}/D_{10}$; $C_c = (D_{30})^2/(D_{10}\times D_{60})$.

TABLE 2 | Oxide analysis and physical characteristics of the tested slag and OPC materials.

Oxide analysis	OPC	Slag (as received)	Physical characteristics	OPC	Slag (as received)
CaO	61.75	41.95	Specific gravity (–)	3.3	2.87
Fe_2O_3	4.89	0.59	Specific surface (cm^2/g)	5,808	7,251
SiO_2	20.21	34.02	Fines (<20 μm, %)	66.3	66.6
Al_2O_3	3.98	15.23	C_u (–)	3.29	9.11
MgO	2.57	6.32	C_c (–)	1.25	1.34
SO_3	1.52	0.19	D_{50} (μm)	17.9	16.8

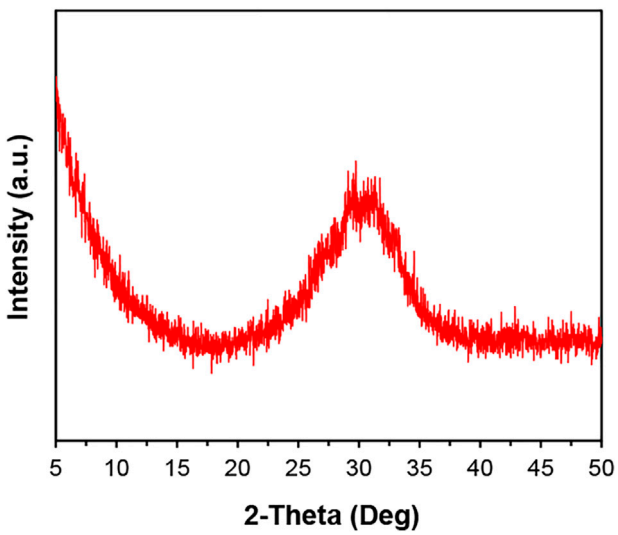

FIGURE 2 | Analysis of XRD profile of the studied slag material.

selected to vary from: 0.26–0.42 for silicate modulus (x_1), 8,000–16000 cm^2/g for slag fineness (x_2) and 0.25–0.45 for activator concentration (x_3), as illustrated in **Table 4**. CCD's experimental results were tailored by using a second order polynomial function, as demonstrated obviously in **Eq. 1**. The mathematical modeling and analysis of variance (ANOVA) were comprehensively carried out by the Design-Expert 11 software.

$$Y = \beta_0 + \sum_{i}^{k} \beta_i X_i + \sum_{i=1}^{k} \beta_{ii} X_i^2 + \sum \sum_{i<j}^{k} \beta_{ij} X_i X_j + \varepsilon \qquad (1)$$

where Y is the anticipated UCS response, X_i and X_j are the points of autonomous factors x_i and x_j, β_0 is the intercept, β_i, β_{ii} and β_{ij} are respectively the linear, quadratic and interaction coefficients, and ε is the associated random error (Pinheiro et al., 2020).

3 RESULTS AND DISCUSSIONS

3.1 Mechanical Assessments

3.1.1 Strength Resistance

3- and 28-day UCS performance of all AAS-CPB mixtures are presented in **Table 3** and **Figure 4**. All AAS-CPB samples, except for 28 day cured E12 sample, exhibit consistently superiority in the strength over CPBs made of OPC, indicating AAS has enormous potential to become an alternative to OPC in the backfill industry. This distinctive disparity in the UCS development can be explained by the difference in cement hydrating products between AAS and OPC. Previous researches (Wang et al., 1994; Wang and Scrivener, 1995; Brough and Atkinson, 2002; Gruskovnjak et al., 2006) have demonstrated that C(N)-A-S-H gel having a high Si/Ca molar ratio is major hydration products for AAS binder.

The strengths of 3 day cured AAS-CPBs range between 0.34 and 1.64, while the strengths of 28 day cured AAS-CPBs are measured in the range of 1.71–3.64 MPa. This significant fluctuation in UCS at both 3- and 28 day curing ages indicates that UCS is significantly affected by the mix composition. At 3 days, E9 with the lowest silicate modulus produces the greatest compressive strength. Meanwhile, the comparison of E9, E10 and E15 which have the same slag fineness and activator concentration indicates that the compressive strength increases with decreasing silicate modulus. The lowest 3 day strength is observed for E11 which has the lowest slag fineness. A comparison of E11and E15 that have the same silicate modulus and activator concentration reveals that an increase in slag fineness from 8,000 cm^2/g to 12000 cm^2/g yields a 197% growth in strength. This finding indicating that increasing slag fineness can improve the mechanical resistance value of AAS-CPB samples at 3 days.

The highest 28 day mechanical resistance is amazingly measured for E13 which has the lowest activator concentration in all the runs. By comparing E13, E14 and E15 which have the same silicate modulus and slag fineness, one can settle that low activator concentration is linked with high strength. It is found, surprisingly, E12 with the highest slag fineness and pretty high 3 day strength shows the lowest strength. This observation shows that the influence of autonomous variables and their connections on UCS is time-dependent.

3.1.2 RSM Modeling

The second order polynomial model (**Eq. 1**) was employed to apt measured UCS results following ANOVA. The ANOVA results for each reliant factor is summarized in **Table 4**. The absence of fit at a major level of 0.05 is employed to certify the aptness of the developed models. The *F*-values for the lack of

TABLE 3 | CCD and determined reliant variables.

Exp no	Autonomous variable blend design						Determined dependent variables	
	Coded			Non-coded			Y_{3d} (MPa)	Y_{28d} (MPa)
	X_1	X_2	X_3	x_1 (–)	x_2 (cm^2/g)	x_3 (–)		
E1	–1	–1	–1	0.30	10,000	0.3	0.84 ± 0.05	2.78 ± 0.11
E2	1	–1	–1	0.38	10,000	0.3	0.56 ± 0.11	3.31 ± 0.14
E3	–1	1	–1	0.30	14,000	0.3	1.29 ± 0.12	2.43 ± 0.08
E4	1	1	–1	0.38	14,000	0.3	0.71 ± 0.08	2.69 ± 0.09
E5	–1	–1	1	0.30	10,000	0.4	0.89 ± 0.07	2.45 ± 0.13
E6	1	–1	1	0.39	10,000	0.4	0.61 ± 0.11	2.64 ± 0.15
E7	–1	1	1	0.30	14,000	0.4	1.58 ± 0.08	2.34 ± 0.23
E8	1	1	1	0.38	14,000	0.4	1.09 ± 0.13	2.01 ± 0.25
E9	–2	0	0	0.26	12,000	0.35	1.64 ± 0.21	2.25 ± 0.21
E10	2	0	0	0.42	12,000	0.35	0.79 ± 0.13	2.51 ± 0.18
E11	0	–2	0	0.34	8,000	0.35	0.34 ± 0.04	2.41 ± 0.07
E12	0	2	0	0.24	16,000	0.35	1.21 ± 0.07	1.71 ± 0.16
E13	0	0	–2	0.34	12,000	0.25	0.67 ± 0.03	3.64 ± 0.07
E14	0	0	2	0.34	12,000	0.45	1.34 ± 0.12	2.44 ± 0.13
E15	0	0	0	0.34	12,000	0.35	1.01 ± 0.16	3.01 ± 0.06
E16	0	0	0	0.21	12,000	0.35	1.06 ± 0.08	2.91 ± 0.05
E17	0	0	0	0.21	12,000	0.35	0.96 ± 0.09	2.94 ± 0.14
E_{OPC}	—	—	—	—	—	—	0.29 ± 0.03	1.95 ± 0.07

[a] x_1: silicate modulus; x_2: slag fineness; x_3: activator concentration.
[b] Y_{3d}: 3 day UCS; Y_{28d}: 28 day UCS.
[c] E_{OPC}, refers to OPC-CPB.

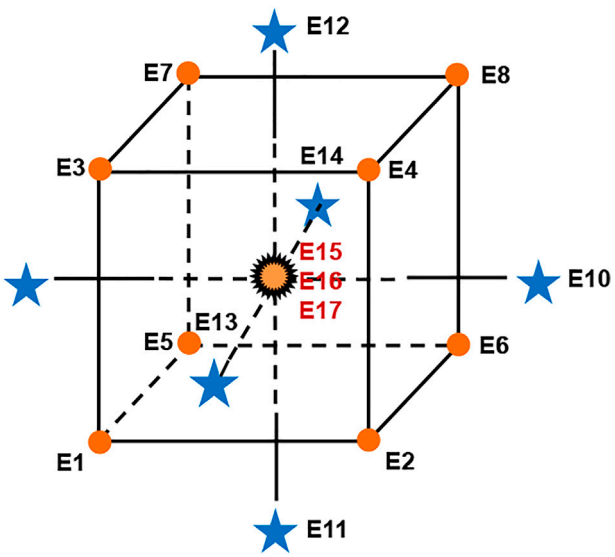

FIGURE 3 | Schematic illustration of CCD (dot in the middle of cube represents three replicates of the center point).

fit were 2.74 for 3 day UCS model and 3.25 for 28 day UCS model, implying that the derived models precisely apt the measured results. The R^2 values of 0.981 and 0.986 for 3-day UCS and 28 day UCS models, respectively, also confirms the good accuracy of the models. Plotting of the predicted values from the models versus the measured results produce perfectly linear curves, as shown clearly in **Figure 5**. All these verify the accuracy and reliability of the response surface models. The significance of all factors including main or quadratic, and their interactions is assessed by using the *p*-value at a significance level of 0.05. The factor is considered statistically substantial if its *p*-value is below 0.05. The predicted models after removing insignificant factors are given by **Eq. 2** for 3 day UCS and **Eq. 3** for 28 day UCS. As shown in **Eqs 2**, **3**, both models are expressed in second order polynomial form and all the linear factors significantly affect the response. For the 3 day UCS model, the slag fineness shows the most significant impact. The higher slag fineness and the lower silicate modulus and activator concentration, the greater the 3 day UCS. Unlike the 3 day UCS model, the most substantial linear variable influencing the 28 day UCS is activator concentration. The 28 day strength is predicted to be positively correlated with all the linear factors. Besides, the quadratic term of activator concentration does not show significant contribution to 3- and 28 day strength.

$$Y_{3d} = 3.71 - 5.6226X_1 + 0.0274X_2 - 0.7679X_3 + 2.1715X_1^2 - 0.0002X_2^2 - 0.0283X_1X_2 + 0.095X_2X_3 \quad (2)$$

$$Y_{28d} = -9.006 + 20.71X_1 + 0.0795X_2 + 4.71X_3 - 6.42X_1^2 - 0.0009X_2^2 - 0.0438X_1X_2 - 15.5X_1X_3 \quad (3)$$

3.1.3 Main and Interactional Effects

3.1.3.1 3 day UCS

To assess the effect of key and interactional variables of autonomous factors on 3 day UCS performance, 3D response-surface schemes are produced, as shown in **Figures 6–8**. These

TABLE 4 | ANOVA of RSM regression analysis.

Term	3 day UCS					28 day UCS				
	Degree-of-freedom	Sum of squares	Average square	*F* Value	*p* Value	Degree-of-freedom	Sum of squares	Average square	*F* Value	*p* Value
Model	9	2.01	0.2233	39.77	<0.0001	9	3.41	0.3785	55.19	<0.0001
X_1	1	0.6931	0.6931	123.42	<0.0001	1	0.0856	0.0856	12.47	0.0096
X_2	1	0.7700	0.7700	137.13	<0.0001	1	0.6045	0.6045	88.14	<0.0001
X_3	1	0.2783	0.2783	49.55	0.0002	1	1.09	1.09	158.46	<0.0001
X_1*X_1	1	0.0462	0.0462	8.23	0.0240	1	0.4045	0.4045	58.97	0.0001
X_2*X_2	1	0.0724	0.0724	12.89	0.0088	1	0.9763	0.9763	142.34	<0.0001
X_3*X_3	1	0.0003	0.0003	0.04	0.8368	1	0.0081	0.0081	1.19	0.3123
X_1*X_2	1	0.0325	0.0325	5.79	0.0470	1	0.078	0.078	11.37	0.0119
X_1*X_3	1	0.0010	0.0010	0.18	0.6839	1	0.1081	0.1081	15.76	0.0054
X_2*X_3	1	0.0406	0.0406	7.23	0.0311	1	0.0066	0.0066	0.96	0.3589
Residual (error)	7	0.0393	0.0056			7	0.0480	0.0069		
Lack of fit	5	0.0343	0.0069	2.74	0.2883	5	0.0427	0.0085	3.25	0.2521
Pure error	2	0.0050	0.0025			2	0.0053	0.0026		
Total	16	2.05				16	3.45			
R^2		0.9808					0.9861			
Adj-R^2		0.9562					0.9682			

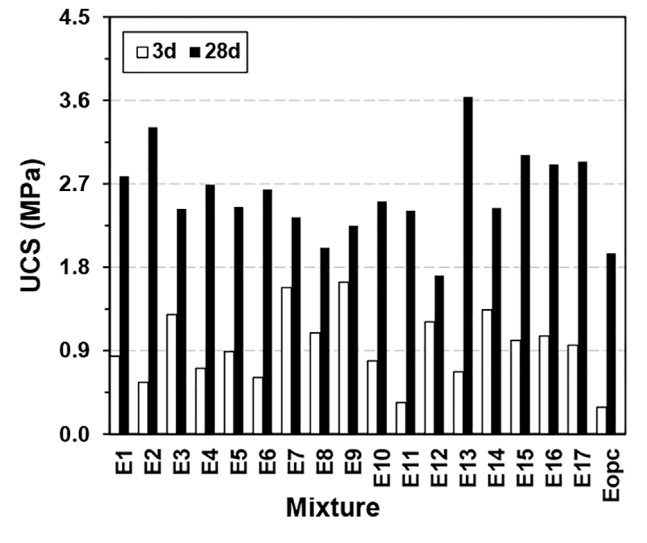

FIGURE 4 | Plots of UCS performance of 3- and 28 day cured CPB samples.

figures also enable us to identify the main trend of UCS development and then predict the optimal direction of UCS.

Figure 6 shows response surface plots of 3 day strength against the slag fineness and silicate modulus at a fixed activator concentration of 0.35. ANOVA shows that the slag fineness is the most significant independent variable influencing the 3 day strength. It is obvious that mixtures with high slag fineness give the greatest strength. Indeed, a higher slag fineness is associated with the increased reactivity and consequently more amount of hydration products (Hallet et al., 2020). The quadratic effect is also significant (**Table 4** and **Figure 6**), but its negative coefficient suggests antagonistic effect on the strength. The effect of slag fineness also depends on the silicate modulus since the interaction between slag fineness and silicate modulus is also significant (**Table 4**). The results presented in **Figure 6** show that the positive effect of MT on 3 day strength become progressively less obvious with increasing silicate modulus suggesting negative contribution of this binary interaction. Therefore, increasing MT while reducing silicate modulus is beneficial to the response.

ANOVA shows that the silicate modulus is the second most significant factor affecting the 3 day strength. As displayed in **Figure 7**, enhanced 3 day strength is observed with the decrease of the silicate modulus and is emphasized by the negative coefficient for the silicate modulus X_1 (**Eq. 2**). This is mainly because a higher pH accelerates the silicon and aluminum dissolved from slag at every-early ages, thereby resulting in more amounts of hydration products. Similar results were also made on other alkali activated materials (Sathonsaowaphak et al., 2009; Ahmari et al., 2012; Sukmak et al., 2013). The quadratic effect is also significant and is expected to increase the 3 day strength with increasing amounts. The outcomes presented in **Figure 8** and **Table 4** suggests that interaction between silicate modulus and activator concentration is negligible.

Figure 8 illustrates the response-surface and contour schemes of 3 day UCS against activator concentration and slag fineness for a silicate modulus of 0.34. Of the linear effects, the activator content is the least weighty (**Table 4**). The highest 3 day strength is achieved when activator content and slag fineness are at high levels while the silicate modulus is held at the level of 0.34. The influence of silicate modulus on the 3 day UCS performance chiefly dependents on level of slag fineness. As slag fineness is high, the increase of activator content enriches the 3 day strength performance, and this positive effect is counteracted with a decrease in slag fineness. This implies that the interaction of activator concentration and slag fineness has a significant effect on the UCS growth.

3.1.3.2 28 day UCS

Response surface and contour plots of 28 day strength were produced against two autonomous factors whereas the third

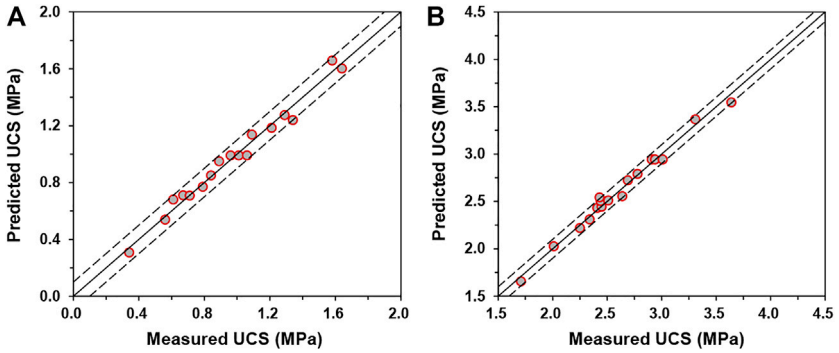

FIGURE 5 | Measured and predicted strengths for 3 day **(A)** and 28 day **(B)** cured AAS-CPB samples.

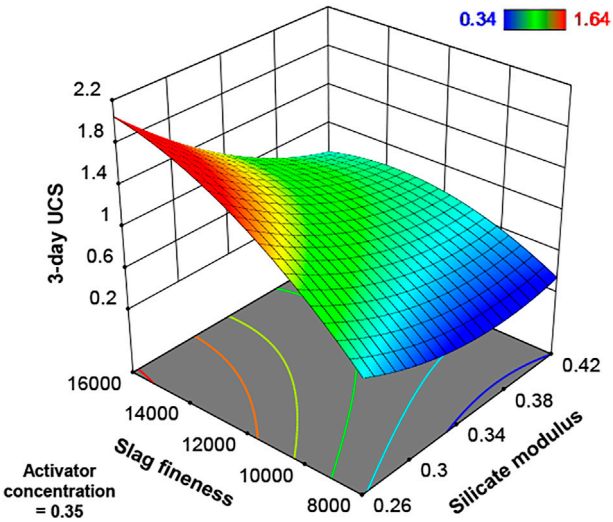

FIGURE 6 | Response-surface of the influence of slag fineness and its interaction with silicate modulus at a fixed activator concentration of 0.35.

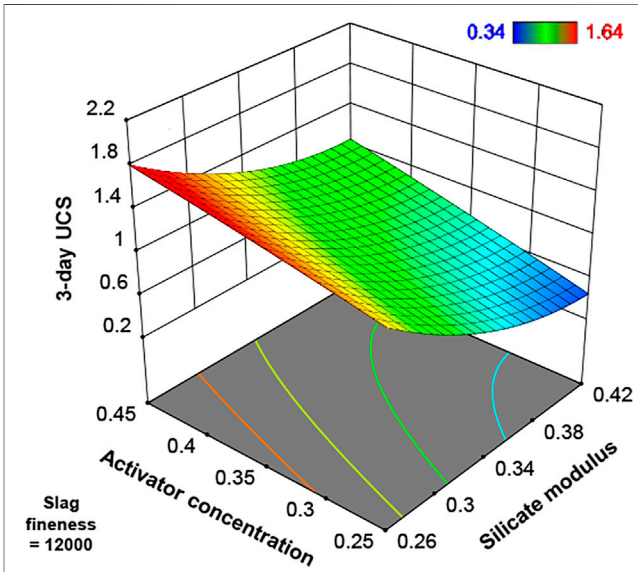

FIGURE 7 | Response-surface of the influence of silicate modulus and its interaction with activator concentration at a fixed slag fineness of 12000 cm^2/g.

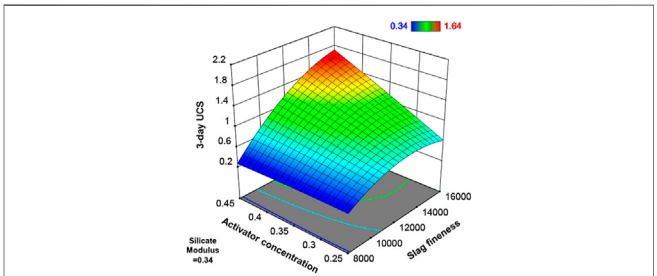

FIGURE 8 | Response-surface of the influence of activator concentration and its interaction with slag fineness for a silicate modulus of 0.34.

one is fixed constantly, as shown in **Figures 9–11**. Comparing the findings of the influence of independent variables on 3 day **6–8** and 28 day UCS (**Figures 9–11**) reveals that the plots for 28 days exhibits patterns different from those for 3 days. This suggests that the level of contribution that the variables on the strength is a function of curing time. ANOVA shows that activator concentration is the most significant independent variable influencing the 28 day UCS. From **Figure 9**, linear effect is observed for the activator concentration in the response surface and counter plots. Contrary to the 3 day strength, the 28 day strength decreases with the increase of activator concentration. Indeed, the increase of alkali promotes the hydration of slag at earlier ages, but excessive alkali will cause the formation of a dense shell surrounding slag particle thereby limiting the late-age hydration of unreacted slag.

In **Table 4** and **Figure 9**, one can observe that there is minor interaction between activator concentration and slag fineness. This indicates that the effect of slag fineness is conditioned by the activator concentration, i.e. the importance of the activator concentration hides the effect of the slag fineness. **Figure 9** shows the plots of the 28-day strength against the slag fineness and silicate modulus for an activator

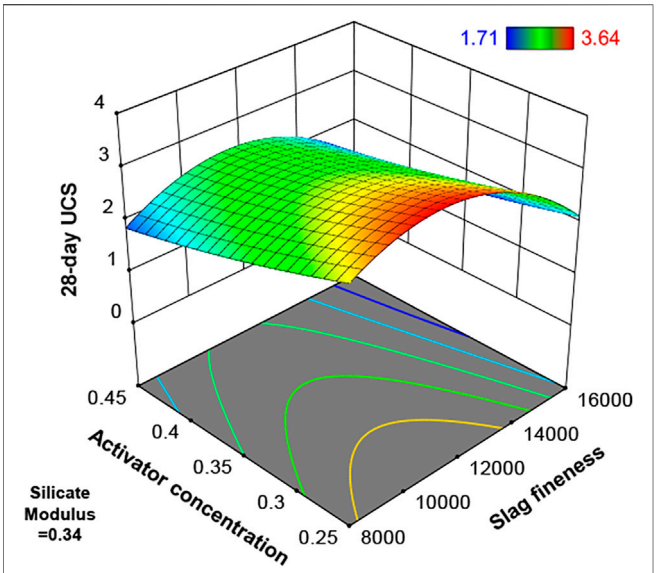

FIGURE 9 | Response-surface of the influence of activator concentration and its interaction with slag fineness for a silicate modulus of 0.34.

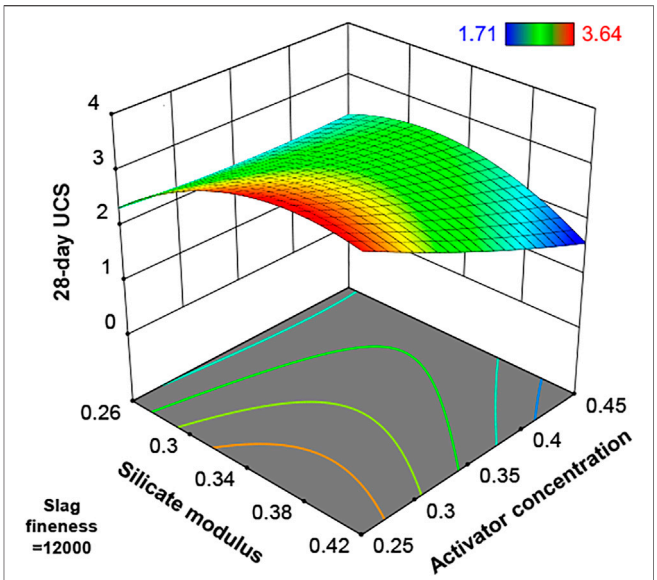

FIGURE 11 | Response-surface of the influence of activator concentration and its interaction with silicate modulus for a slag fineness of 12000 cm^2/g.

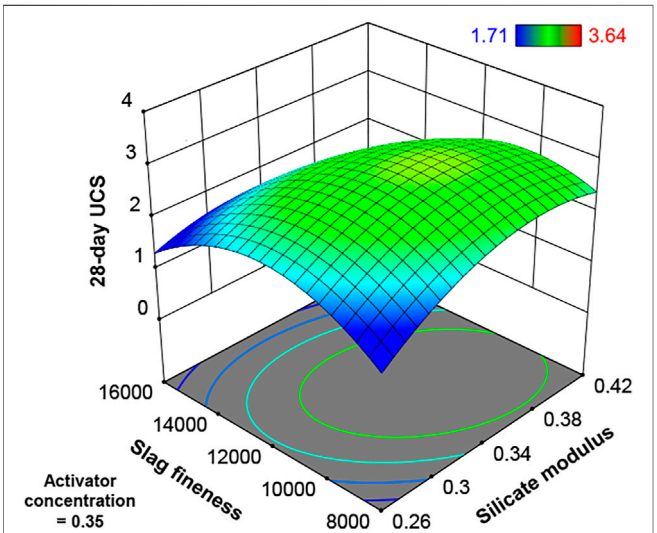

FIGURE 10 | Response-surface of the influence of slag fineness and its interaction with silicate modulus for an activator concentration of 0.35.

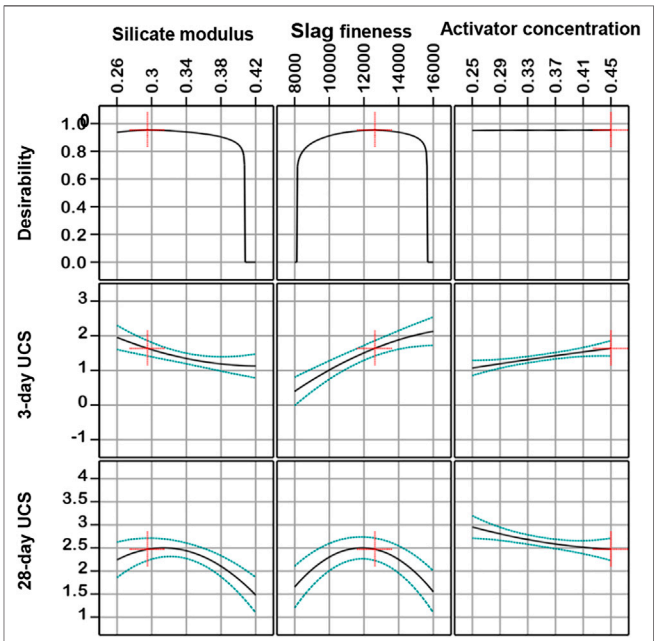

FIGURE 12 | Optimization results of RSM.

concentration = 0.35. As shown in **Table 4**, slag fineness is the second statistically significant factor for the 28 day strength, whereas at 3 days of curing it is of the most significance. This implies that the strength increment with increasing fineness of slag is more pronounced at early age rather than at later ages.

The maximum pattern of 28 day strength as a function of slag fineness and silicate modulus can be clearly seen in **Figure 10**. The 28 day strength is enhanced as the slag fineness increases up to around 10667 cm^2/g; however, the trend reverses with a further increase in the slag fineness. The quadratic effect of the slag fineness appears to be more significant than the corresponding linear effect and the negative coefficient suggests that the favorable effect erodes along with the higher slag fineness. The greatest 28 day strength is obtained around the center of the design from which variations in the slag fineness and/or silicate modulus lead to a reduction in strength. ANOVA also indicates that the binary interaction is statistically significant and has a negative influence on the response.

TABLE 5 | Optimization criteria for AAS-CPB.

Optimize items	Lower limit	Upper limit	Optimization goal
Independent variable			
Silicate modulus	0.26	0.42	—
Slag fineness	8,000	16000	—
Activator concentration	0.25	0.45	—
Response variable			
3 day UCS (MPa)	0.34	1.64	Maximum value
28 day UCS (MPa)	1.71	3.64	Maximum value

ANOVA indicates that the silicate modulus is the factor least statistically relevant. From **Figure 11**, it is obvious that as the silicate modulus increases from 0.26 to 0.42, CPBs experience a gradual increase in the 28 day strength, followed by a decrease. This is because an increase in silica inclines to reduce the hydration rate, causing higher degree of hydration and enriched UCS (Gebregziabiher et al., 2016), and the strength is a result of the competition between the hydration rate and the hydration degree. Moreover, it is found that the level of this transition point depends on activator concentration, i.e. the greater the activator concentration, the lower the transition point level. This funding indicates that there is a strong binary interaction between the silicate modulus and activator concentration.

3.1.4 Response Optimization

The mathematical models between UCS and the independent variables allows finding the optimum combinations that could produce the greatest strength at 3 and 28 days. Equal importance is signed to the optimization goals of 3 day and 28 day UCSs. The optimization criteria are summarized in **Table 5**. The desirability function approach is used for the optimization of the responses. As illustrated in **Figure 12**, the mixture with a combination of independent variables of silicate modulus = 0.295, slag fineness = 12630.2 cm^2/g, activator concentration = 0.45 (denoted as $E_{optimal}$) gives the optimum responses. The 3 day and 28 day strength is predicted as 1.64 and 2.47 MPa respectively with a global desirability of 0.955.

4 CONCLUSION

According to the results obtained from tests and analyses, following conclusions can be drawn:

✓ The magnitude of input that autonomous variables on UCS is a function of time. The most significant variables influencing 3- and 28 day UCS are slag fineness and activator concentration, respectively.

✓ Increasing hydration reaction area and the pH of pore solution favors the strength development at the very early ages. However, it is found that excessive alkali leads to the formation of a dense shell surrounding slag particle, thus reducing the strength acquisition at later ages.

✓ The mix proportion giving the optimal responses is silicate modulus = 0.295, slag fineness = 12630.2 cm^2/g, activator concentration = 0.45 with a forecast 3- and 28 day UCS of 1.64 and 2.47 MPa, respectively.

The CCD-based RSM is proved to be a reliable tool for the optimization of AAS-CPB synthesis. This methodology can be of great use in practice since there are fairly strong interactions among the components of AAS-CPB. In addition, the technical information of this investigation will be beneficial for the design of durable, cost-effective and sustainable AAS-CPB.

DATA AVAILABILITY STATEMENT

The original contributions presented in the study are included in the article/Supplementary Material, further inquiries can be directed to the corresponding authors.

AUTHOR CONTRIBUTIONS

All authors listed have made a substantial, direct and intellectual contribution to the work, and approved it for publication.

FUNDING

The authors would like to acknowledge the funding by the National Natural Science Foundation of China (grant number 51804063) and the Fundamental Research Funds for the Central Universities (grant number N2101043) is sincerely acknowledged by the writers for its generous support this research project.

REFERENCES

Abdollahnejad, Z., Luukkonen, T., Mastali, M., Kinnunen, P., and Illikainen, M. (2019). Development of One-Part Alkali-Activated Ceramic/Slag Binders Containing Recycled Ceramic Aggregates. *J. Mater. Civ. Eng.* 31, 04018386. doi:10.1061/(asce)mt.1943-5533.0002608

Ahmari, S., Zhang, L., and Zhang, J. (2012). Effects of Activator Type/concentration and Curing Temperature on Alkali-Activated Binder Based on Copper Mine Tailings. *J. Mater. Sci.* 47, 5933–5945. doi:10.1007/s10853-012-6497-9

AnuragKumar, R., Goyal, S., and Srivastava, A. (2021). A Comprehensive Study on the Influence of Supplementary Cementitious Materials on Physico-Mechanical, Microstructural and Durability Properties of Low Carbon Cement Composites. *Powder Tech.* 394, 645–668. doi:10.1016/j.powtec.2021.08.081

Aydın, S., and Baradan, B. (2012). Mechanical and Microstructural Properties of Heat Cured Alkali-Activated Slag Mortars. *Mater. Des.* 35, 374–383. doi:10.1016/j.matdes.2011.10.005

Behera, S. K., Mishra, D. P., Singh, P., Mishra, K., Mandal, S. K., Ghosh, C. N., et al. (2021). Utilization of Mill Tailings, Fly Ash and Slag as Mine Paste Backfill Material: Review and Future Perspective. *Construction Building Mater.* 309, 125120. doi:10.1016/j.conbuildmat.2021.125120

Belem, T., and Benzaazoua, M. (2008). Design and Application of Underground Mine Paste Backfill Technology. *Geotech. Geol. Eng.* 26, 147–174. doi:10.1007/s10706-007-9154-3

Benzaazoua, M., Fall, M., and Belem, T. (2004). A Contribution to Understanding the Hardening Process of Cemented Pastefill. *Minerals Eng.* 17, 141–152. doi:10.1016/j.mineng.2003.10.022

Benzaazoua, M., Ouellet, J., Servant, S., Newman, P., and Verburg, R. (1999). Cementitious Backfill with High Sulfur Content Physical, Chemical, and Mineralogical Characterization. *Cement Concrete Res.* 29, 719–725. doi:10.1016/S0008-8846(99)00023-X

Bilim, C., Karahan, O., Atiş, C. D., and İlkentapar, S. (2013). Influence of Admixtures on the Properties of Alkali-Activated Slag Mortars Subjected to Different Curing Conditions. *Mater. Des.* 44, 540–547. doi:10.1016/j.matdes.2012.08.049

Brough, A. R., and Atkinson, A. (2002). Sodium Silicate-Based, Alkali-Activated Slag Mortars - Part I. Strength, Hydration and Microstructure. *Cement Concrete Res.* 32, 865–879. doi:10.1016/S0008-8846(02)00717-2

Cao, S., Xue, G., and Yilmaz, E. (2019a). Flexural Behavior of Fiber Reinforced Cemented Tailings Backfill under Three-Point Bending. *IEEE Access* 7, 139317–139328. doi:10.1109/access.2019.2943479

Cao, S., Yilmaz, E., Song, W., and Xue, G. (2019b). Assessment of Acoustic Emission and Triaxial Mechanical Properties of Rock-Cemented Tailings Matrix Composites. *Adv. Mater. Sci. Eng.* 2019, 1–12. doi:10.1155/2019/6742392

Cavusoglu, I., Yilmaz, E., and Yilmaz, A. O. (2021). Sodium Silicate Effect on Setting Properties, Strength Behavior and Microstructure of Cemented Coal Fly Ash Backfill. *Powder Tech.* 384, 17–28. doi:10.1016/j.powtec.2021.02.013

Cihangir, F., Ercikdi, B., Kesimal, A., Deveci, H., and Erdemir, F. (2015). Paste Backfill of High-Sulphide Mill Tailings Using Alkali-Activated Blast Furnace Slag: Effect of Activator Nature, Concentration and Slag Properties. *Minerals Eng.* 83, 117–127. doi:10.1016/j.mineng.2015.08.022

Cihangir, F., Ercikdi, B., Kesimal, A., Ocak, S., and Akyol, Y. (2018). Effect of Sodium-Silicate Activated Slag at Different Silicate Modulus on the Strength and Microstructural Properties of Full and Coarse Sulphidic Tailings Paste Backfill. *Construction Building Mater.* 185, 555–566. doi:10.1016/j.conbuildmat.2018.07.105

Dai, C., Wu, A., Qi, Y., and Chen, Z. (2019). The Optimization of Mix Proportions for Cement Paste Backfill Materials via Box-Behnken Experimental Method. *J. Inst. Eng. India Ser. D* 100, 307–316. doi:10.1007/s40033-019-00180-7

El-Wafa, M. A., and Fukuzawa, K. (2018). Early-Age Strength of Alkali-Activated Municipal Slag–Fly Ash–Based Geopolymer Mortar. *J. Mater. Civ. Eng.* 30, 04018040. doi:10.1061/(asce)mt.1943-5533.0002234

Ercikdi, B., Baki, H., and İzki, M. (2013). Effect of Desliming of Sulphide-Rich Mill Tailings on the Long-Term Strength of Cemented Paste Backfill. *J. Environ. Manage.* 115, 5–13. doi:10.1016/j.jenvman.2012.11.014

Ercikdi, B., Cihangir, F., Kesimal, A., Deveci, H., and Alp, İ. (2009a). Utilization of Industrial Waste Products as Pozzolanic Material in Cemented Paste Backfill of High Sulphide Mill Tailings. *J. Hazard. Mater.* 168, 848–856. doi:10.1016/j.jhazmat.2009.02.100

Ercikdi, B., Kesimal, A., Cihangir, F., Deveci, H., and Alp, İ. (2009b). Cemented Paste Backfill of Sulphide-Rich Tailings: Importance of Binder Type and Dosage. *Cement and Concrete Composites* 31, 268–274. doi:10.1016/j.cemconcomp.2009.01.008

Fall, M., Benzaazoua, M., and Saa, E. G. (2008). Mix Proportioning of Underground Cemented Tailings Backfill. *Tunnelling Underground Space Tech.* 23, 80–90. doi:10.1016/j.tust.2006.08.005

Fall, M., Célestin, J. C., Pokharel, M., and Touré, M. (2010). A Contribution to Understanding the Effects of Curing Temperature on the Mechanical Properties of Mine Cemented Tailings Backfill. *Eng. Geology.* 114, 397–413. doi:10.1016/j.enggeo.2010.05.016

Gao, Y., Xu, J., Luo, X., Zhu, J., and Nie, L. (2016). Experiment Research on Mix Design and Early Mechanical Performance of Alkali-Activated Slag Using Response Surface Methodology (RSM). *Ceramics Int.* 42, 11666–11673. doi:10.1016/j.ceramint.2016.04.076

Gebregziabiher, B. S., Thomas, R. J., and Peethamparan, S. (2016). Temperature and Activator Effect on Early-Age Reaction Kinetics of Alkali-Activated Slag Binders. *Construction Building Mater.* 113, 783–793. doi:10.1016/j.conbuildmat.2016.03.098

Gruskovnjak, A., Lothenbach, B., Holzer, L., Figi, R., and Winnefeld, F. (2006). Hydration of Alkali-Activated Slag: Comparison with Ordinary Portland Cement. *EMPA Act.* 34, 119–128. doi:10.1680/adcr.2006.18.3.119

Guo, Z., Qiu, J., Jiang, H., Zhang, S., and Ding, H. (2021). Improving the Performance of Superfine-Tailings Cemented Paste Backfill with a New Blended Binder. *Powder Tech.* 394, 149–160. doi:10.1016/j.powtec.2021.08.029

Hajkowicz, S. A., Heyenga, S., and Moffat, K. (2011). The Relationship between Mining and Socio-Economic Well Being in Australia's Regions. *Resour. Pol.* 36, 30–38. doi:10.1016/j.resourpol.2010.08.007

Hallet, V., De Belie, N., and Pontikes, Y. (2020). The Impact of Slag Fineness on the Reactivity of Blended Cements with High-Volume Non-ferrous Metallurgy Slag. *Construction Building Mater.* 257, 119400. doi:10.1016/j.conbuildmat.2020.119400

Hefni, M., and Hassani, F. (2021). Effect of Air Entrainment on Cemented Mine Backfill Properties: Analysis Based on Response Surface Methodology. *Minerals* 11, 81–18. doi:10.3390/min11010081

Helinski, M., Fahey, M., and Fourie, A. (2007). Numerical Modeling of Cemented Mine Backfill Deposition. *J. Geotech. Geoenviron. Eng.* 133, 1308–1319. doi:10.1061/(asce)1090-0241(2007)133:10(1308)

Jafari, M., Shahsavari, M., and Grabinsky, M. (2020). Experimental Study of the Behavior of Cemented Paste Backfill under High Isotropic Compression. *J. Geotech. Geoenvironmental Eng.* 146, 06020019. doi:10.1061/(asce)gt.1943-5606.0002383

Jafari, M., Shahsavari, M., and Grabinsky, M. (2021). Drained Triaxial Compressive Shear Response of Cemented Paste Backfill (CPB). *Rock Mech. Rock Eng.* 54, 3309–3325. doi:10.1007/s00603-021-02464-5

Jiang, H., and Fall, M. (2017). Yield Stress and Strength of saline Cemented Tailings in Sub-zero Environments: Portland Cement Paste Backfill. *Int. J. Mineral Process.* 160, 68–75. doi:10.1016/j.minpro.2017.01.010

Jiang, H., Han, J., Li, Y., Yilmaz, E., Sun, Q., and Liu, J. (2020). Relationship between Ultrasonic Pulse Velocity and unconfined compressive strength for Cemented Paste Backfill with Alkali-Activated Slag. *Nondestructive Test. Eval.* 35, 359–377. doi:10.1080/10589759.2019.1679140

Jiang, H., Qi, Z., Yilmaz, E., Han, J., Qiu, J., and Dong, C. (2019). Effectiveness of Alkali-Activated Slag as Alternative Binder on Workability and Early Age Compressive Strength of Cemented Paste Backfills. *Construction Building Mater.* 218, 689–700. doi:10.1016/j.conbuildmat.2019.05.162

Kesimal, A., Ercikdi, B., and Yilmaz, E. (2003). The Effect of Desliming by Sedimentation on Paste Backfill Performance. *Minerals Eng.* 16, 1009–1011. doi:10.1016/S0892-6875(03)00267-X

Köken, E., and Lawal, A. I. (2021). Investigating the Effects of Feeding Properties on Rock Breakage by Jaw Crusher Using Response Surface Method and Gene Expression Programming. *Adv. Powder Tech.* 32, 1521–1531. doi:10.1016/j.apt.2021.03.007

Koohestani, B., Darban, A. K., Darezereshki, E., Mokhtari, P., Yilmaz, E., and Yilmaz, E. (2018). The Influence of Sodium and Sulfate Ions on Total Solidification and Encapsulation Potential of Iron-Rich Acid Mine Drainage in Silica Gel. *J. Environ. Chem. Eng.* 6, 3520–3527. doi:10.1016/j.jece.2018.05.037

Koohestani, B., Mokhtari, P., Yilmaz, E., Mahdipour, F., and Darban, A. K. (2021). Geopolymerization Mechanism of Binder-free Mine Tailings by Sodium Silicate. *Construction Building Mater.* 268, 121217. doi:10.1016/j.conbuildmat.2020.121217

Korde, C., Cruickshank, M., West, R. P., and Pellegrino, C. (2019). Activated Slag as Partial Replacement of Cement Mortars: Effect of Temperature and a Novel Admixture. *Construction Building Mater.* 216, 506–524. doi:10.1016/j.conbuildmat.2019.04.172

Li, J., Yilmaz, E., and Cao, S. (2021). Influence of Industrial Solid Waste as Filling Material on Mechanical and Microstructural Characteristics of Cementitious Backfills. *Construction Building Mater.* 299, 124288. doi:10.1016/j.conbuildmat.2021.124288

Luukkonen, T., Abdollahnejad, Z., Yliniemi, J., Kinnunen, P., and Illikainen, M. (2018). One-part Alkali-Activated Materials: A Review. *Cement Concrete Res.* 103, 21–34. doi:10.1016/j.cemconres.2017.10.001

Oraon, B., Majumdar, G., and Ghosh, B. (2006). Application of Response Surface Method for Predicting Electroless Nickel Plating. *Mater. Des.* 27, 1035–1045. doi:10.1016/j.matdes.2005.01.025

Ouattara, D., Mbonimpa, M., Yahia, A., and Belem, T. (2018). Assessment of Rheological Parameters of High Density Cemented Paste Backfill Mixtures Incorporating Superplasticizers. *Construction Building Mater.* 190, 294–307. doi:10.1016/j.conbuildmat.2018.09.066

Palanikumar, K. (2007). Modeling and Analysis for Surface Roughness in Machining Glass Fibre Reinforced Plastics Using Response Surface Methodology. *Mater. Des.* 28, 2611–2618. doi:10.1016/j.matdes.2006.10.001

Pinheiro, C., Rios, S., Viana da Fonseca, A., Fernández-Jiménez, A., and Cristelo, N. (2020). Application of the Response Surface Method to Optimize Alkali Activated Cements Based on Low-Reactivity Ladle Furnace Slag.

Construction Building Mater. 264, 120271. doi:10.1016/j.conbuildmat.2020.120271

Rakhimova, N. R., and Rakhimov, R. Z. (2015). Alkali-activated Cements and Mortars Based on Blast Furnace Slag and Red clay brick Waste. *Mater. Des.* 85, 324–331. doi:10.1016/j.matdes.2015.06.182

Rana, N. M., Ghahramani, N., Evans, S. G., McDougall, S., Small, A., and Take, W. A. (2021). Catastrophic Mass Flows Resulting from Tailings Impoundment Failures. *Eng. Geology.* 292, 106262. doi:10.1016/j.enggeo.2021.106262

RenaYadav, S., Yadav, S., Killedar, D. J., Kumar, S., and Kumar, R. (2022). Eco-innovations and Sustainability in Solid Waste Management: An Indian Upfront in Technological, Organizational, Start-Ups and Financial Framework. *J. Environ. Manage.* 302, 113953. doi:10.1016/j.jenvman.2021.113953

Saedi, M., Behfarnia, K., and Soltanian, H. (2019). The Effect of the blaine Fineness on the Mechanical Properties of the Alkali-Activated Slag Cement. *J. Building Eng.* 26, 100897. doi:10.1016/j.jobe.2019.100897

Sathonsaowaphak, A., Chindaprasirt, P., and Pimraksa, K. (2009). Workability and Strength of lignite Bottom Ash Geopolymer Mortar. *J. Hazard. Mater.* 168, 44–50. doi:10.1016/j.jhazmat.2009.01.120

Simms, P., and Grabinsky, M. (2009). Direct Measurement of Matric Suction in Triaxial Tests on Early-Age Cemented Paste Backfill. *Can. Geotech. J.* 46, 93–101. doi:10.1139/T08-098

Simon, D., and Grabinsky, M. (2013). Apparent Yield Stress Measurement in Cemented Paste Backfill. *Int. J. Mining, Reclamation Environ.* 27, 231–256. doi:10.1080/17480930.2012.680754

Soto-Pérez, L., López, V., and Hwang, S. S. (2015). Response Surface Methodology to Optimize the Cement Paste Mix Design: Time-dependent Contribution of Fly Ash and Nano-Iron Oxide as Admixtures. *Mater. Des.* 86, 22–29. doi:10.1016/j.matdes.2015.07.049

Sukmak, P., Horpibulsuk, S., and Shen, S.-L. (2013). Strength Development in clay-fly Ash Geopolymer. *Construction Building Mater.* 40, 566–574. doi:10.1016/j.conbuildmat.2012.11.015

Sun, Q., Tian, S., Sun, Q., Li, B., Cai, C., Xia, Y., et al. (2019). Preparation and Microstructure of Fly Ash Geopolymer Paste Backfill Material. *J. Clean. Prod.* 225, 376–390. doi:10.1016/j.jclepro.2019.03.310

Sun, Q., Wei, X., Li, T., and Zhang, L. (2020). Strengthening Behavior of Cemented Paste Backfill Using Alkali-Activated Slag Binders and Bottom Ash Based on the Response Surface Method. *Materials* 13, 855. doi:10.3390/ma13040855

Tariq, A., and Yanful, E. K. (2013). A Review of Binders Used in Cemented Paste Tailings for Underground and Surface Disposal Practices. *J. Environ. Manage.* 131, 138–149. doi:10.1016/j.jenvman.2013.09.039

Turner, L. K., and Collins, F. G. (2013). Carbon Dioxide Equivalent (CO2-e) Emissions: A Comparison between Geopolymer and OPC Cement concrete. *Construction Building Mater.* 43, 125–130. doi:10.1016/j.conbuildmat.2013.01.023

Wang, S.-D., and Scrivener, K. L. (1995). Hydration Products of Alkali-Activated Slag Cement. *Cement Concrete Res.* 25, 561–571. doi:10.1016/0008-8846(95)00045-E

Wang, S.-D., Scrivener, K. L., and Pratt, P. L. (1994). Factors Affecting the Strength of Alkali-Activated Slag. *Cement Concrete Res.* 24, 1033–1043. doi:10.1016/0008-8846(94)90026-4

Wu, A., Wang, Y., Wang, H., Yin, S., and Miao, X. (2015). Coupled Effects of Cement Type and Water Quality on the Properties of Cemented Paste Backfill. *Int. J. Mineral Process.* 143, 65–71. doi:10.1016/j.minpro.2015.09.004

Xue, G., Yilmaz, E., Song, W., and Cao, S. (2020). Fiber Length Effect on Strength Properties of Polypropylene Fiber Reinforced Cemented Tailings Backfill Specimens with Different Sizes. *Construction Building Mater.* 241, 118113. doi:10.1016/j.conbuildmat.2020.118113

Yang, J., Sun, Z., Li, B., Ji, Y., and Hu, K. (2019). Measuring Volume Change of Alkali-Activated Slag Pastes in Early Stage by Using Helium Pycnometry. *J. Mater. Civ. Eng.* 31, 06019011. doi:10.1061/(asce)mt.1943-5533.0002900

Yang, L., Xu, W., Yilmaz, E., Wang, Q., and Qiu, J. (2020). A Combined Experimental and Numerical Study on the Triaxial and Dynamic Compression Behavior of Cemented Tailings Backfill. *Eng. Structures* 219, 110957. doi:10.1016/j.engstruct.2020.110957

Yilmaz, E., Belem, T., Benzaazoua, M., Kesimal, A., Ercikdi, B., and Cihangir, F. (2011). Use of High-Density Paste Backfill for Safe Disposal of Copper/zinc Mine Tailings. *Gospod. Surowcami Miner./Miner. Resour. Manag.* 27, 81–94.

Yuan, B., Yu, Q. L., and Brouwers, H. J. H. (2015). Reaction Kinetics, Reaction Products and Compressive Strength of Ternary Activators Activated Slag Designed by Taguchi Method. *Mater. Des.* 86, 878–886. doi:10.1016/j.matdes.2015.07.077

Zaibo, Z., Juanhong, L., Aixiang, W., and Hongjiang, W. (2021). Coupled Effects of Superplasticizers and Glazed Hollow Beads on the Fluidy Performance of Cemented Paste Backfill Containing Alkali-Activated Slag and MSWI Fly Ash. *Powder Technol.* 399, 116726. doi:10.1016/j.powtec.2021.08.012

Zhang, L., and Yue, Y. (2018). Influence of Waste Glass Powder Usage on the Properties of Alkali-Activated Slag Mortars Based on Response Surface Methodology. *Construction Building Mater.* 181, 527–534. doi:10.1016/j.conbuildmat.2018.06.040

Zhang, S., Ren, F., Zhao, Y., Qiu, J., and Guo, Z. (2021). The Effect of Stone Waste on the Properties of Cemented Paste Backfill Using Alkali-Activated Slag as Binder. *Construction Building Mater.* 283, 122686. doi:10.1016/j.conbuildmat.2021.122686

Zhao, Y., Taheri, A., Karakus, M., Chen, Z., and Deng, A. (2020). Effects of Water Content, Water Type and Temperature on the Rheological Behaviour of Slag-Cement and Fly Ash-Cement Paste Backfill. *Int. J. Mining Sci. Tech.* 30, 271–278. doi:10.1016/j.ijmst.2020.03.003

Zheng, J., Tang, Y., and Feng, H. (2021). Utilization of Low-Alkalinity Binders in Cemented Paste Backfill from Sulphide-Rich Mine Tailings. *Construction Building Mater.* 290, 123221. doi:10.1016/j.conbuildmat.2021.123221

Zhou, N., Zhang, J., Ouyang, S., Deng, X., Dong, C., and Du, E. (2020). Feasibility Study and Performance Optimization of Sand-Based Cemented Paste Backfill Materials. *J. Clean. Prod.* 259, 120798. doi:10.1016/j.jclepro.2020.120798

Zhu, L., Jin, Z., Zhao, Y., and Duan, Y. (2021a). Rheological Properties of Cemented Coal Gangue Backfill Based on Response Surface Methodology. *Construction Building Mater.* 306, 124836. doi:10.1016/j.conbuildmat.2021.124836

Zhu, Y., Wang, Z., Li, Z., and Yu, H. (2022b). Experimental Research on the Utilization of Gold Mine Tailings in Magnesium Potassium Phosphate Cement. *J. Building Eng.* 45, 103313. doi:10.1016/j.jobe.2021.103313

Conflict of Interest: The authors declare that the research was conducted in the absence of any commercial or financial relationships that could be construed as a potential conflict of interest.

Publisher's Note: All claims expressed in this article are solely those of the authors and do not necessarily represent those of their affiliated organizations, or those of the publisher, the editors and the reviewers. Any product that may be evaluated in this article, or claim that may be made by its manufacturer, is not guaranteed or endorsed by the publisher.

Copyright © 2022 Dai, Ren, Gu, Yilmaz, Fang and Jiang. This is an open-access article distributed under the terms of the Creative Commons Attribution License (CC BY). The use, distribution or reproduction in other forums is permitted, provided the original author(s) and the copyright owner(s) are credited and that the original publication in this journal is cited, in accordance with accepted academic practice. No use, distribution or reproduction is permitted which does not comply with these terms.